ELSEVIER

Ecological Modelling 145 (2001) 129–142

ECOLOGICAL MODELLING

www.elsevier.com/locate/ecolmodel

Simulating vertical and horizontal multifractal patterns of a longleaf pine savanna

J.B. Drake [a,b], J.F. Weishampel [a,*]

[a] *Department of Biology, University of Central Florida, Orlando, FL 32816-2368, USA*
[b] *Department of Geography, University of Maryland, College Park, MD 20742, USA*

Received 16 August 2000; received in revised form 16 May 2001; accepted 22 May 2001

Abstract

Many ecological processes (e.g., individual growth, competition, and mortality) are dictated by existing spatial patterns and lead to the generation of new spatial conditions. Spatial patterns are the result of a spectrum of ecological processes operating at widely different time scales. In this study, a cellular automata model that incorporated autecological information for longleaf pine (LLP) and fire effects was used to simulate one- and two-dimensional spatial canopy/gap properties (i.e., the distribution of crown heights and widths) over a savanna landscape. These were quantified using multifractal analysis and were compared to remotely-sensed data from LLP stands from the Disney Wilderness Preserve located near Kissimmee, Florida. Lidar-derived transect information provided canopy height patterns and aerial photography provided crown width and horizontal distribution patterns. Multifractal spectra and size class distributions were found to be sensitive to spatially interactive parameters (i.e., competition, fire ignition and spread probabilities). Simulations with moderate levels of competition coupled with a relatively high fire frequency (once every 4 years) and a relatively high likelihood of fire spread across five-meter grid cells (dependent on litter fuel loads) were shown to create patterns that closely mimic the quasi three-dimensional remotely-sensed measures of this open canopy system.

Keywords: Canopy/gap; Cellular automata; Fire regime; Laser altimetry; Longleaf pine; Multifractal; Spatial pattern

1. Introduction

Presently, less than 2% of the original 33 million ha of longleaf pine (LLP) (*Pinus palustris*) forests in the southeastern United States remain (Schwartz, 1999). Since 1936, LLP forests, once the most abundant land cover category in Florida, have declined by 90% (Kautz, 1998) primarily due to clearing for agriculture or development as well as conversion to other pine species. Moreover, fire suppression policies during the early half of the 20th century greatly hindered natural LLP regeneration and promoted the establishment of hardwood and more aggressive southern pine species (Brockway and Lewis, 1997; McCay, 2000).

Because ecological pattern and process (Watt, 1947) or structure and function (Shugart, 1996; Spies, 1998) are convolved, understanding the

* Corresponding author. Tel.: +1-407-823-6634; fax: +1-407-823-5769.
E-mail address: jweisham@mail.ucf.edu (J.F. Weishampel).

0304-3800/01/$ - see front matter
PII: S0304-3800(01)00398-2

spatial organization of forests lends insight to the underlying dynamic mechanisms that produce the landscape morphology and its subsequent biophysical properties and behaviors (Pielke et al., 1998). The physiognomy of LLP forests is best described as a savanna consisting of tree clumps or scattered individuals not forming a continuous canopy (Platt, 1999) thereby providing desirable habitat for jeopardized vertebrate populations such as the Red-cockaded Woodpecker (*Picoides borealis*), fox squirrel (*Sciurus niger*), and flatwood salamander (*Ambystoma cingulatum*). As a result, the density and size of LLP trees, the frequency and size of open space, and the scale of aggregation have been measured to define LLP stands (Noel et al., 1998; Gilliam and Platt, 1999). Thus, empirical and mechanistic landscape modeling approaches (see examples in Mladenoff and Baker (1999)) may provide a basis for predicting spatial dynamics to facilitate LLP forest restoration and conservation management efforts.

Spatial patterns in terrestrial ecosystems are largely a result of the interactions of numerous biotic and abiotic processes operating at widely different spatiotemporal scales. Hence, reductionistic modeling (Friend et al., 1997) approaches may be inappropriate to capture broad-scale dynamics of these systems. Instead, simple rule-based cellular automata (CA) models may provide a better template for understanding of the underlying processes that influence these spatial patterns (Lett et al., 1999). For example, Solé and Manrubia (1995) explored the spatial dynamics of species-rich tropical rainforest with a generic single species, CA gap-type model. Similarly, Chen et al. (1990), Drossel and Schwabl (1992), and Holling et al. (1996) developed simple forest-fire models and evaluated the sensitivity of parameters on self-organized critical behavior.

Here, our focus was to use a single species CA model based on the autecology of LLP to explore spatial patterns of LLP stands resulting from major biotic (i.e., intraspecific competition) and abiotic (i.e., fire) interactions. The variable spatial nature of savannas, characterized with both one-dimensional height measurements from lidar transects and two-dimensional canopy/gap (binary) data from aerial photography over a second-growth LLP savanna was compared to the simulated patterns. As savanna ecosystems represent a domain poised between grasslands and woodlands, these simulations may also help to elucidate processes that promote this structurally distinct state.

2. Methods

2.1. Description of study area and remotely-sensed data

The Scanning Lidar Imager of Canopies by Echo Recovery (SLICER) laser profiling system acquired data after leaf off in November 1995 from the Disney Wilderness Preserve (DWP) near Kissimmee, Florida. The DWP is a ≈ 4600 ha former cattle ranch managed by The Nature Conservancy that typifies the remaining undeveloped regions of central Florida. The terrain is relatively flat. The vegetation consists of wetland patches (e.g., marshes, bayhead swamps, and cypress domes) found in depressions surrounded by a matrix of more xeric upland, pine and scrubby flatwood communities. Conceived in the early 1990s as a mitigation site for wetland disturbance by the Walt Disney World Corporation and the Greater Orlando Aviation Authority, the DWP has undergone extensive hydrological/vegetation restoration consisting of filling in drainage canals and reestablishing a normal fire regime.

The SLICER sensor was developed at NASA Goddard Space Flight Center to provide geolocated, high-resolution (i.e., 11 cm) measurements of vertical vegetation structure and ground elevations beneath dense canopies (Harding et al., 1994; Blair and Harding, 1998; Lefsky et al., 1999). When recording information from a forest, SLICER produces a waveform whose first and last returns above background noise represent the canopy top and the ground, respectively. Intervening returns correspond to the distribution of intervening canopy surfaces (Weishampel et al., 1996).

For this mission, SLICER was flown aboard the NASA Wallops Flight Facility T-39 Sabreliner aircraft. The laser pulses consisted of five

across-track circular footprints 10–12 m in diameter nominally spaced 10 m along and across the flight track. Footprint diameter is a function of the beam divergence and the altitude of the plane. The aircraft ground speed and pulse repetition rate defined footprint spacing. Though a previous study analyzed the waveform properties of forested vegetation and accuracy of canopy height estimates at the DWP (Weishampel et al., 1997), this study focuses solely on horizontal spatial patterns of canopy height, i.e., the difference in elevations between the first and the last return.

Six, one-dimensional canopy height profiles from the upland flatwood communities were derived from segments of 50 contiguous, along-track footprints from the two outer and middle SLICER transects. Canopy heights were extracted using software developed by Lefsky et al. (1999) for ground detection. Comparisons of spatial patterns of laser-derived and field measured estimates of canopy height for these transect are found in Drake and Weishampel (2000). Two-dimensional patterns, canopy/gap locations were obtained from 1993 color infrared, 2 m resolution aerial photographs over the DWP. Eight 500×500 m^2 (25 ha) savanna areas classified as pine flatwood, or scrubby flatwood covertypes were arbitrarily selected from the overall image. These areas were converted to a binary format that segmented the image into canopy and ground for analysis in a similar manner as Prihodko et al. (1994).

2.2. Spatially-explicit longleaf pine savanna model

The rules which define the CA model used in this study (the 'savanna game' or SG), were derived from previous studies of the interactions and dynamics of LLP. These are somewhat comparable to those in another CA model (the 'forest game' or FG) used to simulate multifractal patterns of a tropical rainforest canopy (Solé and Manrubia, 1995). The empirical studies used to develop the ecological relationships in the SG model focused on competitive and fire effects on LLP of different age classes. Juvenile LLPs are found in discrete clumps scattered among more randomly distributed adult trees in an old-growth stand (Platt et al., 1988). Local neighborhoods have a pronounced effect on the distribution of saplings and juveniles (Grace and Platt, 1995; Palik et al., 1997) with clumps of young trees occurring in locations more distant from large pines than expected by chance (Rathbun and Cressie, 1994). Thus, although early studies (Platt et al., 1988) proposed that fire was the primary mechanism for producing the observed patterns in pine savannas, it now seems that both fire and intraspecific competitive interactions play a crucial role in determining these spatial patterns (Noel et al., 1998).

The simulated landscape consisted of a 100×100 grid of 5×5 m^2 cells (i.e., 25 ha) to correspond with the binary images. To avoid edge effects, the landscape was wrapped around itself to form a torus. The landscape was initialized by randomly planting saplings or activating a portion of the total cells. The default probability of a sapling occurring on a cell was 0.5, but the model proved to be insensitive to initial conditions. One-dimensional transects from the model were produced by aggregating the 5×5 m^2 grid cells into 10×10 m^2 blocks, so that 50 blocks corresponded to the 500 m field and lidar-derived transects. In addition, model-generated trees that were within the error range of the altimeter measurement (i.e., ≈ 1.5 m tall or 5 cm diameter at breast height) were not considered. The rules that affected changes between states (e.g., gap to tree) and within states (e.g., tree growth) are illustrated in a general diagram (Fig. 1) and are detailed below.

2.2.1. Rule 1. Tree growth

Trees grew in terms of height (H) asymptotically approaching a maximum height (H_{max}). Following allometric relationships from Platt et al. (1988), growth was sigmoidal (i.e., more rapid at earlier ages then decreasing as the maximum size was approached).The equation for the annual increment vertical growth (G_v) in meters was:

$$G_v = G_h(1 - H/H_{max}), \quad (1)$$

where G_h was a growth multiplier that varied between 0 and 1. Maximum height was a constant of 40 m (inferred from Platt et al., 1988). Tree growth was reduced by competitive interactions (C_n) with neighbors (Section 2.2.2) and was in-

creased immediately following a nearby fire event dependent on the fire intensity (Platt, 1999) following:

$$G_h = \left(\frac{C_n + E_f}{2}\right)\left(1 - \frac{H}{H_{max}}\right), \quad (2)$$

where C_n was a function of the sizes of neighboring trees (Section 2.2.2). Enhancement from fire (E_f) was an exponential saturation function of the amount of nearby burnt litter (L_b) during the year of a fire:

$$E_f = 1 - e^{\left(-\sum L_b/N_f\right)}, \quad (3)$$

where ΣL_b is the sum of burnt litter in the 3×3 focal neighborhood ($N_f = 9$).

For comparison with the aerial photography, crown diameters were also simulated. Crown diameter increases were based on growth relationships derived for slash pine (*Pinus elliottii*) by Dean and Jokela (1992) which are comparable to LLP crown measures recorded by Brockway and Outcalt (1998). Because the 5×5 m^2 cells were either occupied or unoccupied with a one tree per cell maximum, crown diameter growth (G_c) was a step function where

$$G_c = \begin{cases} 1 \text{ cell} & \text{if } 12 < H \leqslant 0 \text{ m} \\ 2 \text{ cells} & \text{if } 20 < H \leqslant 25 \text{ m} \\ 3 \text{ cells} & \text{if } H > 25 \text{ m}. \end{cases} \quad (4)$$

These discrete crown diameter steps correspond to when $> 50\%$ of the area in a cell or cells would be filled based the continuous Dean and Jokela (1992) relationship. For the situation where the crown center was not the center of a grid cell (i.e., where G_c equaled 2 cells) the 2×2 cell crown was randomly placed in one of the four possible orientations.

2.2.2. Rule 2. Competition

Resource availability (R) was a function of the neighboring tree sizes that in turn affected mortality (Section 2.2.6). Trees of different size classes (i.e., juveniles, subadults, and adults) were affected in different ways. Neighboring (i.e., within a two cell radius) adult and subadult trees suppressed tree growth regardless of size class, whereas juvenile neighbors only affected juvenile growth (following Rathbun and Cressie, 1994; Grace and Platt, 1995). The equation for resource availability was:

$$R = \left[1 - \frac{\sum H_n}{\left(\frac{H_{max}}{CI}\right)}\right]((2N_r + 1)^2 - 1), \quad (5)$$

where ΣH_n was the sum of adult and subadult tree heights or heights of trees taller than the focal tree in the neighborhood. CI was a competition index (CI) whose default value was two. The neighborhood radius (N_r), the distance of influen-

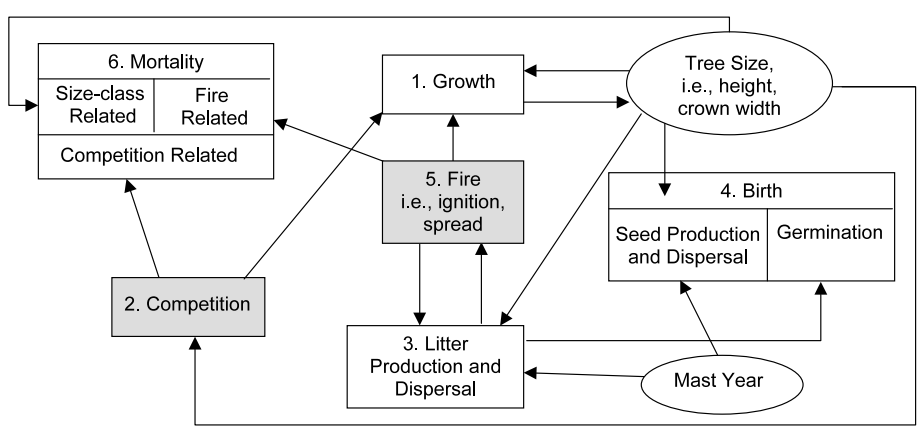

Fig. 1. General relationships among components of the SG. Processes are represented by rectangles, states by ovals. Spatially-explicit parameters in the gray boxes were analyzed for sensitivity.

tial cells around a focal cell was set at two for these simulations. Resource availability could range from zero to one. Zero indicated the least amount of resources. For the default CI, resource availability would reach zero when all trees in the neighborhood achieved half of their maximum height.

2.2.3. Rule 3. Litterfall

Leaf litter fall was a step function of tree size and distance from tree. The amount of litter falling each year was represented by an integer (1–3). Approximately every other year trees copiously dropped litter. The timing of such an event was stochastically determined. During such a year, adult trees dispersed litter in a two-cell radius including diagonals around and (unlike seed dispersal) within the focal cell. Subadults dispersed litter in a one-cell radius around and within the focal cell. More litter fell directly beneath the tree and decreased by one in cells further away from the source tree. During a regular year, adult trees dispersed needles in a one-cell radius and beneath the tree, and subadults dispersed needles only in the focal cell. Litter on a cell could be from multiple tree sources; it accumulated annually until burned by a fire and did not decompose.

2.2.4. Rule 4. Birth

Seed production was a function of tree size and whether or not it was a mast year. Seeds endured only one annual time step. Juveniles (i.e., $\leqslant 12.5$ m tall) were unable to produce offspring (Platt et al., 1988). Adults (i.e., $\geqslant 22$ m tall) produced roughly four times as many seeds as subadults (i.e., between 12.5 and 22 m). The probability of a seed landing on a nearby cell (P_s) was:

$$P_s = 1 - e^{-0.2(H_{max} - H)}. \quad (6)$$

During episodic mast events estimated as occurring every 5–10 years (Platt et al., 1988; Rathbun and Cressie, 1994), recruitment nearly quadrupled. The maximum number of seeds produced by an adult and a subadult during a mast year was 80 and 32, respectively, versus 32 and 8 in a regular year.

Dispersal around subadults and adults was limited to neighborhoods one and two cells away including diagonals, respectively, around the source tree during non-episodic years. During episodic years, dispersal ranged from two to three cells deep for subadults and adults, respectively. Seed number decreased in cells further away from the source tree. For each seed in a cell, germination probability (P_g) was a negative exponential function of the amount of litter present (L) in a particular cell and only happened in cells without trees:

$$P_g = e^{-(0.5L)/2}. \quad (7)$$

When germination occurred, a 1 m tall sapling was established in the cell. Although many seeds (80 maximum) could exist in a cell for a given year, only one sapling could occupy a cell. Thus, the higher the number of seeds in a cell, the higher the probability of germination.

2.2.5. Rule 5. Fire effects

Fires were ignited stochastically on the SG landscape either by lightning striking an adult tree or by spreading in from the edge of the 25 ha region. After the initial trees on the landscape matured (i.e., becoming sufficiently tall to function as a lightning attractor), the probability of a lightning strike or edge spread event was fairly even. Fires occur in LLP savannas on the order of 3–5 years. This was simulated with the default fire probability (FP) of 0.25 for a given year. Fires could only occur once a year. Both fire intensity and the probability of fire spread across the SG landscape were a function of the amount of fuel (i.e., litter) present. Because litter could accumulate infinitely in theory, these were modeled with asymptotic relationships. The probability of fire spreading (F_s) to an adjacent unburned cell (located in cardinal directions) was a hyperbolic power function of litter amount (L):

$$F_s = 0.1 + 0.9(L^3/(SR^3 + L^3)), \quad (8)$$

where the spread resistance parameter (SR) was estimated. Though litter moisture was not explicitly modeled, a higher SR would correspond to wetter conditions. Without litter, fire had a 0.1 probability of spreading across a 5×5 m^2 cell.

With the default *SR* equaling two, a 95 percent chance of fire spread across a cell occurred after an accumulation of 5 litter units. Thus, the extent and the shape of the burn scar were stochastically determined.

2.2.6. Rule 6. Mortality

Tree mortality was a function of competition, fire, and other natural causes. Competition-related mortality (M_c) used the resource availability formula derived above (Eq. (5)); however, it was reduced immediately after a fire event where litter in the vicinity was burned (Eq. (3)). If $R + E_f - 1 < 0$, we used:

$$M_c = 1 - e^{(R + E_f - 1)}, \tag{9}$$

otherwise $M_c = 0$. Fire-related mortality (M_f) was a function of fire intensity and tree size. Fire intensity was a function of accumulated litter in a cell that reached its maximum at 14 litter units:

$$M_f = (1 - e^{-L})\ e^{0.2(-H+1)}. \tag{10}$$

Hence, fire-induced mortality was common among juvenile trees and rare among subadult and adult trees. In addition, ambient mortality due to natural, nonmodeled forces (e.g., disease, hurricanes, windthrows, etc.) was most prominent in both juveniles and very old adult trees. Following Platt et al. (1988), juveniles were given a 0.05 mortality probability, subadults were given a 0.01 mortality probability, and adults were given a linearly increasing mortality probability up to 0.06 with increasing size.

2.3. Multifractal analysis of spatial patterns

Fractal (Lorimer et al., 1994; Vedyushkin 1994) and multifractal (Schuering and Riedi, 1994; Cheng and Agterberg, 1995; Solé and Manrubia, 1995; Cheng 1997; Drake, 1998; Drake and Weishampel, 2000) techniques have been used to characterize non-Euclidean spatial pattern of trees and forested systems. Fractal techniques are based on the idea that any measure assigned to an object is dependent on the scale or resolution that is considered. Typically, fractal measures detail changes over a variety of different resolutions. A box counting approach (e.g., Schuering and Riedi, 1994) is often utilized to calculate the fractal dimension (D_f), i.e.,

$$D_f = \lim_{\varepsilon \to 0} \left(\frac{1}{q-1} \right) \frac{\log \sum_{i=1}^{N(\varepsilon)} p_i^q(\varepsilon)}{\log(\varepsilon)}, \tag{11}$$

where $N(\varepsilon)$ is the number of boxes of size ε needed to cover the object and $p_i(\varepsilon)$ is the measure contained in the i-th box of size ε and q is a scaling exponent. For a simple fractal, $q = 0$.

However, natural forested systems are not merely fractal; they are multifractal (Cheng and Agterberg, 1995; Solé and Manrubia, 1995; Drake and Weishampel, 2000). Thus, they exhibit multiple scaling regions and are therefore not self-similar as denoted by the presence of residuals in the log–log regression line associated with Eq. (11) (see review in Ricotta (2000)). The scaling exponent, q, represents infinite possibilities, i.e., from $-\infty$ to $+\infty$. To calculate multifractal spectra from the remotely-sensed and simulated one and two-dimensional LLP patterns, we followed the box-counting fixed-size algorithm of Mach et al. (1995) using software that we developed. Multifractal spectra, i.e., $\alpha(q)$ versus $f(q)$ or α versus $f(\alpha)$ plots, were generated following:

$$\alpha(q) = \lim_{\varepsilon \to 0} \frac{E\left(\sum_{i=1}^{N(\varepsilon)} \hat{p}_i(\varepsilon) \log p_i(\varepsilon) \right)}{\log \varepsilon} \tag{12}$$

and

$$f(q) = \lim_{\varepsilon \to 0} \frac{E\left(\sum_{i=1}^{N(\varepsilon)} \hat{p}_i(\varepsilon) \log \hat{p}_i(\varepsilon) \right)}{\log \varepsilon}, \tag{13}$$

where

$$\hat{p}_i(\varepsilon) = \frac{p_i^q(\varepsilon)}{\sum_{j=1}^{N(\varepsilon)} p_j^q(\varepsilon)}, \tag{14}$$

and $E(\ )$ is the expectation.

This technique of multifractal analysis has been depicted as changing the zoom and field of view of a microscope over a pattern (Appleby, 1996). Thus, through the examination of multifractal measures, subtle differences in spatial patterns in natural systems can be explored. Fine-scale patterns embedded within coarser patterns may

Table 1
Range of values tested for spatially-sensitive parameters

Parameter	Default	Low	High
Competition (CI)	2	0.5	10
Fire Probability (FP)	0.25	0.02	0.5
Fire Spread Resistance (SR)	2	1	40

reflect ecological processes operating at different spatiotemporal scales such as competition and fire-mediated disturbance.

2.4. Simulation experiments

To understand the basic model behavior in terms of size class distribution and spatial patterns of tree heights and crowns, we ran the model for 2000 years using defaults values (shown in Table 1). The default values represent our best estimate as to how the system works. These values are not based on empirical information or calibration exercises. To assess the sensitivity of model-generated spatial patterns to estimated parameters that functionally link gridcells, we ran the simulations with a range of values for CI, FP, and SR. Higher values of CI correspond to higher competition. Higher values of FP correspond to a higher fire frequency on the landscape. Higher values of SR correspond to a reduced chance of fire spread from one cell to the next. Though not explicitly modeled here, connectivity of fuel loads across a landscape (related to SR) is a function of FP, i.e., simulations with high FP values have disconnected fuel loads (Miller and Urban, 2000). Because the model has stochastic properties, simulations were run ten times for each parameter value. Model-generated and remotely-sensed multifractal patterns for one-dimensional height distributions and two-dimensional canopy/gap locations were compared. For the one-dimensional analysis taller trees represent an increase in mass, i.e., $p_i(\varepsilon)$, for a given window of size ε and the $f(\alpha)$ spectra range between 0 and 1. For the two-dimensional analysis, only the presence/absence of canopy for a 5×5 m^2 cell was assessed; hence the $f(\alpha)$ spectra range between 1 and 2.

3. Results

3.1. Model behavior

The SG model was run for 2000 years using the default values listed in Table 1. This was done to verify that it yielded reasonable results relating to LLP heights and canopy/gap spatial patterns, as well as to determine when the model reaches a quasi-stable state (i.e., free from initialization biases). LLP distributions by size class for 600 years (Fig. 2) revealed that the numbers of adults and subadults did not change greatly after 100 years, but juveniles increased in numbers until year 350. After this time, fire and competitive factors allowed the system to equilibrate in terms of size class distributions. In terms of summed tree height which correlates to biomass, the landscape reached a 'steady state' after 150 years, after which minor fluctuations were due to stochastic fire and mortality effects.

Another way to visualize this development was through analysis of model-produced canopy spatial patterns using multifractal analyzes (Fig. 3) through time. These analyzes are based on the crown heights in randomly selected 10×500 m^2 transects within the 25 ha landscape. At 50 years, the range of the $f(\alpha)$ spectrum was reduced compared with subsequent years. The monofractal dimensions as represented by the apex of the parabolic spectra are relatively stable (≈ 0.8) up to 1000 years. After which there was a significant drop that may relate to a sparse distribution of crowns immediately after a large fire. Such fluctuations were less evident when examining two-dimensional crown patterns. This technique revealed that a quasi-stable state in spatial patterns was reached within 500 years. As such, subsequent patterns analyzed in this study were from obtained at year 500.

3.2. Sensitivity to spatially interactive parameters

3.2.1. Effect of competition

The CI from Eq. (6) was systematically varied to analyze results from low (CI = 0.5) and high

(CI = 10) competition scenarios. Patterns of crowns/gaps (Fig. 4) and tree size distributions (Fig. 5(a)) from high and low competition systems were noticeably distinct. Higher competitive interactions result in a decrease in juvenile trees, and a more self-similar distribution of tree heights. As a result, increased competition also results in multifractal spectra (Fig. 5(b)) with less overall spread, an indicator of self-similarity (Solé and Manrubia, 1995; Mandelbrot and Evertsz, 1991). Variance around the high competition one-dimensional tree height multifractal pattern was large compared to that with low competition. In terms of canopy/gap distributions, greater competition also resulted in an overall reduction in number of LLP canopies, and, therefore, produced a lower apex associated with the multifractal measures (Fig. 5(c)). The two-dimensional multifractal patterns were less variable than the one-dimensional patterns.

3.2.2. Effect of fire frequency

Scenarios of high (0.5) and low (0.02) probabilities of a fire occurring in a given year (or approximately every 2 or 50 years, respectively) produced different tree size distributions and patterns of canopies/gaps. Though larger trees appear to be more clumped in the low fire frequency Fig. 4 example, differences in the spatial patterns of crowns were generally not as evident as found with competition. This was also apparent by examining the slight differences in the multifractal spectra based on the crown distributions (Fig. 6(c)). Higher fire probabilities resulted in many more juvenile trees (Fig. 6(a)). The number of juveniles with low fire frequency was about half as found with the low competition scenario. This reduction is due to litter accumulation. LLP needs bare mineral soil for germination. Lower fire probabilities resulted in higher levels of self-similarity in canopy height as illustrated by a collapsing multifractal spectrum (Fig. 6(b)).

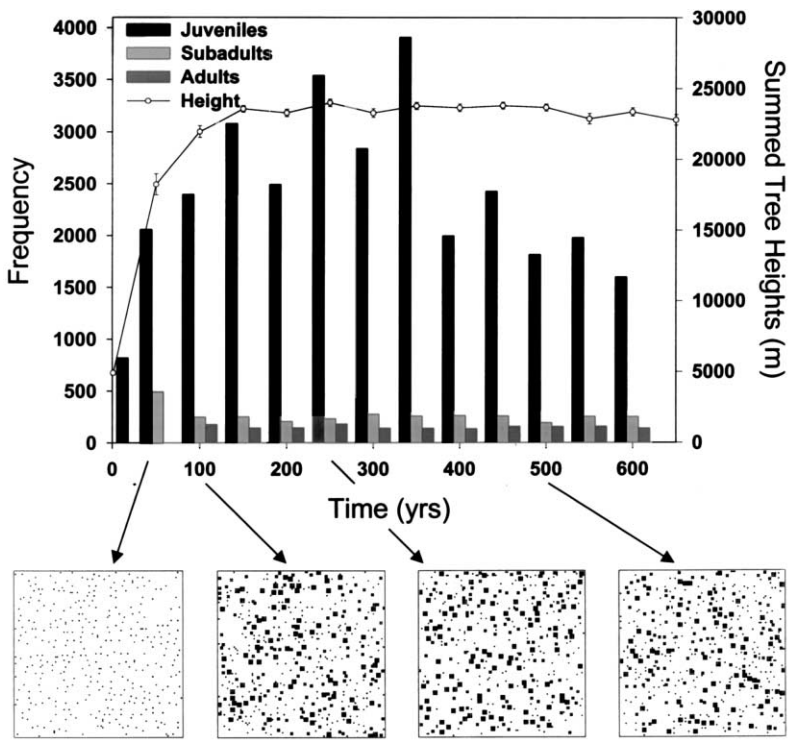

Fig. 2. Average simulated size class distributions for juvenile (height $\leqslant$ 12.5 m), subadult (12.5–22 m), and adult ($\geqslant$ 22 m) LLP trees and the overall summed tree heights in a 25 ha area through time. The lower panels depict the dynamic spatial crown patterns.

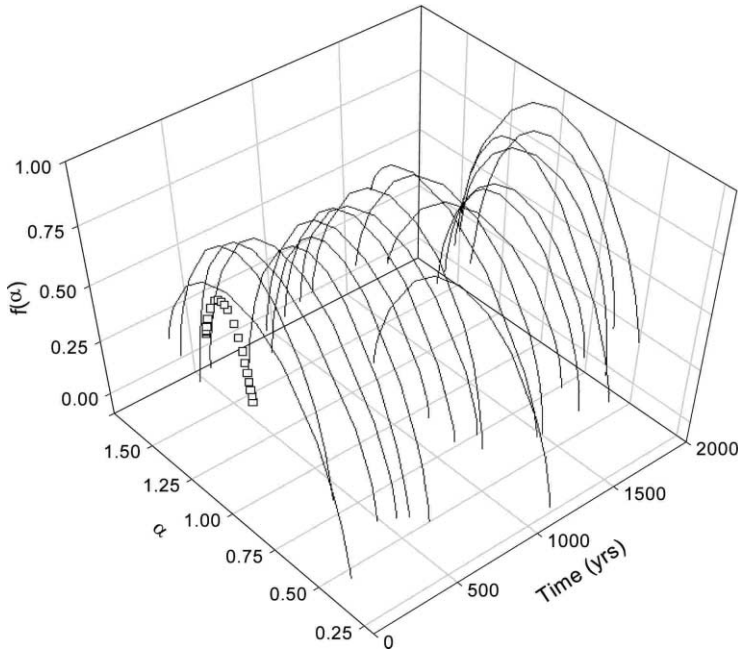

Fig. 3. Multifractal spectra of LLP height patterns from randomly selected 10×100 m^2 belt transects over a 2000 year span. The time at 50 years is designated by the open squares.

Additionally, lower fire probabilities also resulted in a noticeable increase in variability of multifractal spectra for both tree height and canopy/gap distributions. This variability was largely a result of how long after a fire event the 'snapshots' of tree height and canopy/gap distributions were taken. Because rare fire events tend to be large, there can be dramatic differences from one time step to the next.

3.2.3. Effect of spread probability

In terms of size class distribution, scenarios of high (SR = 1) and low (SR = 40) fire spread probability (Eq. (8)) were comparable to those for high and low fire frequency, respectively. However, in terms of one- and two-dimensional spatial patterns, high and low probabilities of fire spread were more comparable to low and high competitive effects, respectively. Lower fire spread resulted in a more evenly distributed, self-similar distribution of tree sizes (Fig. 7(a) and (b)); however, the distribution of canopy and gap elements were still highly multifractal (Fig. 7(c)) as evidenced by a large spectral spread. These patchy patterns were the result of highly isolated fire events, and therefore result in unique local fractal properties that were elucidated through the multifractal analysis.

3.3. Comparison with remotely-sensed data

The final step in this study compared patterns from the SG model with default parameter values to remotely patterns from a LLP savanna. These values were not calibrated to fit the patterns found in the remotely-sensed data. In order to make this assessment, one-dimensional tree height transects from the SLICER instrument and two-dimensional canopy/gap distributions derived from the aerial photography DWP were utilized.

Patterns of tree height distributions along transects from both the SG model and lidar-derived measurements showed very similar responses. The multifractal spectra (Fig. 8(a)) were nearly identical in terms of overall spread and variation with a mono-fractal dimension slightly greater than 0.8.

Similarly, patterns of canopy/gap distributions from the default SG model and aerial photography have remarkably similar multifractal (Fig. 8(b)) patterns. The monofractal values were 1.7.

The departure from total self-similarity revealed in these plots, seen both in their respective multifractal plots, is nearly identical for all scales for the modeled and remotely-sensed patterns. This divergence from total self-similarity is what makes these patterns multifractal, and is characteristic of underlying nonlinear mechanisms (Solé and Manrubia, 1995).

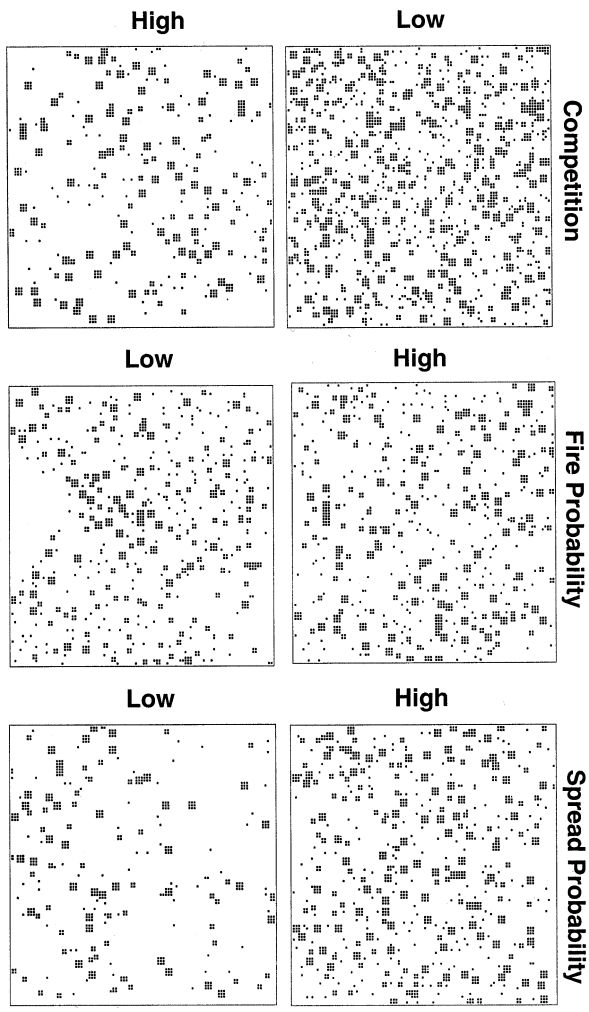

Fig. 4. Randomly chosen two-dimensional examples of simulated LLP crown patterns at year 500 for 500×500 m^2 area for different CI, FP, and SR values.

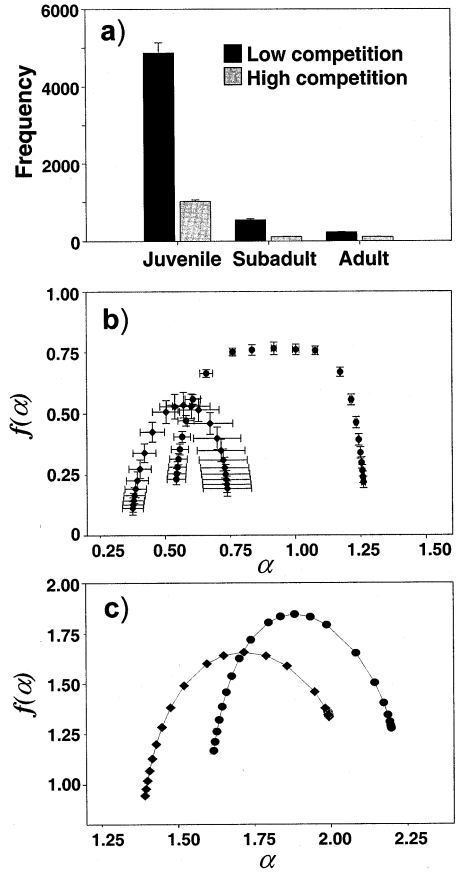

Fig. 5. Effects of competition on (a) size class distributions, (b) multifractal spectra of one-dimensional tree height patterns, and (c) two-dimensional crown patterns. For the multifractal spectra high and low competition are designated by ◆ and ●, respectively. Extensions from bars and markers (that are barely visible in c) represent standard error for ten simulations.

4. Discussion

Multifractal properties (e.g., $f(\alpha)$ spectra) are not calculated simply because dimensions are intrinsically interesting, but when coupled with models, they represent a potential window to the pattern generating mechanisms (Mandelbrot, 1988). In this study, underlying biotic and abiotic processes influenced state changes between canopy and gap, and among different height classifications; the multifractal patterns produced by these changes are indicators of the non-equi-

librium, dynamic nature of LLP savannas. Subsets of a savanna ecosystem that are in different states represent different local conditions, each with their own unique fractal properties. As such, multifractal analysis helped to explore the dynamic patterns that are produced by the CA model. When the model parameters were adjusted, it was possible to illustrate how important ecological processes influenced spatial structure and heterogeneity in LLP savannas.

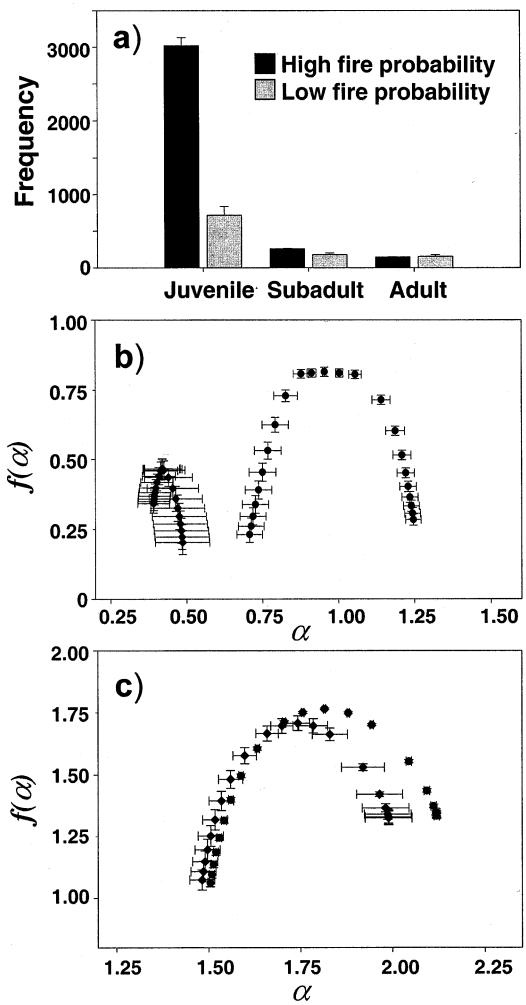

Fig. 6. Effects of fire ignition probability on (a) size class distributions, (b) multifractal spectra of one-dimensional tree height patterns, and (c) two-dimensional crown patterns. For the multifractal spectra low and high fire probabilities are designated by ◆ and ●, respectively. Extensions from bars and markers represent standard error for ten simulations.

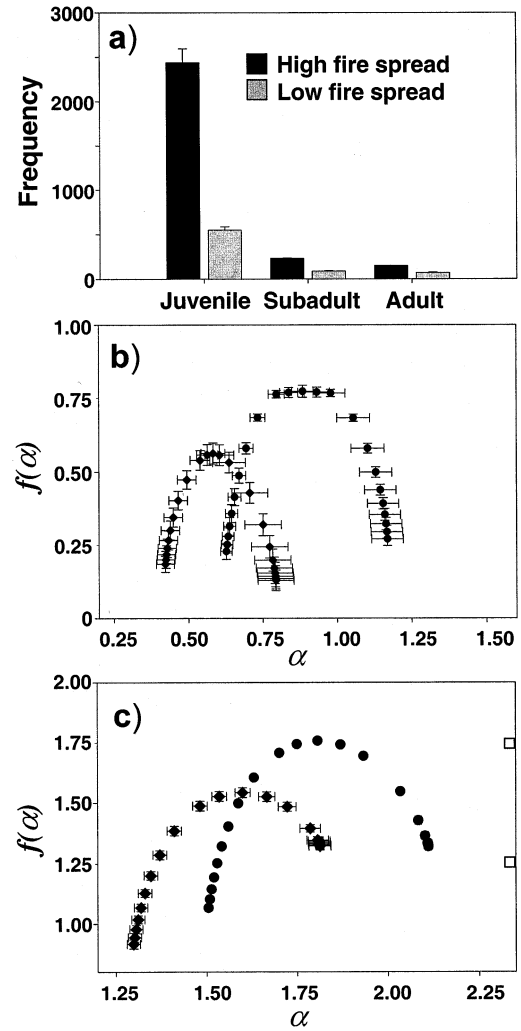

Fig. 7. Effects of fire spread on (a) size class distributions, (b) multifractal spectra of one-dimensional tree height patterns, and (c) two-dimensional crown patterns. For the multifractal spectra low and high spread probabilities are designated by ◆ and ●, respectively. Extensions from bars and markers represent standard error for ten simulations.

Through subtle changes to simple fire and competition parameters, the model produced remarkably different landscapes with unique spatial properties. If these were adjusted to extreme values (i.e., no fire ignition and low competition) the landscape exhibited a closed-canopy state. Therefore based on this model, patterns that are char-

acteristic of a savanna domain are most likely maintained, at least in part, by fire and competitive processes. This corresponds to empirical studies that demonstrated that both fire (Platt et al., 1988) and competitive (Grace and Platt, 1995; Palik et al., 1997; Noel et al., 1998) processes are paramount in forming spatial patterns in LLP savannas. This model further supported the belief that frequent growing-season fires (i.e., once every 4 years) ignited by lightning that are spread by pyrogenic vegetation, coupled with significant competitive interactions (Grace and Platt, 1995) are responsible for the persistence of LLP savannas (Platt 1999). We have illustrated how a simple CA model based on these major processes can reproduce similar spatial patterns to an actual LLP savanna.

Although the spatial patterns of tree heights and canopy/gap locations in a LLP savanna may also be influenced by other abiotic factors (e.g., heterogeneity in nutrient/water availability, hurricane disturbances, etc.), it is important to note that even with changes to only these two key processes the CA model was able to reproduce savanna-esque structure that mirrored the observed patterns. Because the elimination/reduction of fire and competition resulted in a closed-canopy landscape, it is also clear that the complex interaction between these processes is crucial in maintaining LLP savanna spatial patterns.

Spatial patterns of LLP trees are not only important intraspecifically, but also affect other species as well. LLP is a 'driver' species (Holling et al., 1996) which determines the overall behavior and structure of southeastern United States pine savanna ecosystems. Because competition and fire processes are important in creating and maintaining the spatial patterns of LLP trees, they also have an indirect but substantial impact on all savanna flora and fauna.

Acknowledgements

We thank: the Laser Altimeter Processing Facility at NASA GSFC for the laser profiling data; TNC's DWP for GIS coverages, aerial photography, and use of their preserve; and Jack Stout and Hank Whittier for reviews of earlier versions of the manuscript. The NASA Mission to Planet Earth New Investigator Program (NAG-W5202), National Science Foundation Career Award (DEB-9984574), and the University of Central Florida Office of Sponsored Research provided financial support.

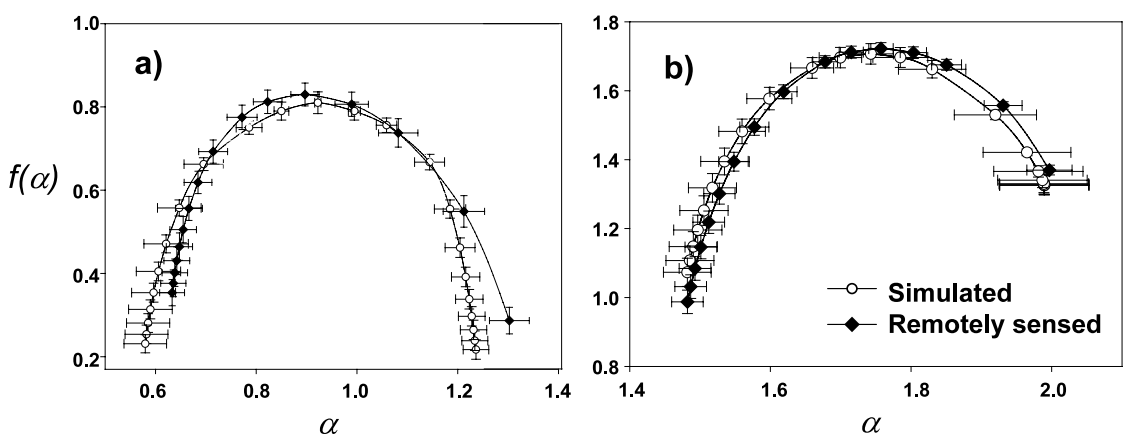

Fig. 8. Comparison between simulated and remotely-sensed multifractal spectra for (a) one- and (b) two-dimensional crown data. Extensions from markers represent ± standard error for six lidar transects, eight binary images from aerial photography, and ten simulations.

References

Appleby, S., 1996. Multifractal characterization of the distribution pattern of the human population. Geog. Anal. 28, 147–160.

Blair, J.B., Harding, D., 1998. Laser remote sensing branch—SLICER available at: http://ltpwww.gsfc.nasa.gov/eib/slicer.html.

Brockway, D.G., Lewis, C.E., 1997. Long-term effects of dormant-season prescribed fire on plant community diversity, structure and productivity in a longleaf pine wiregrass ecosystem. Forest Ecol. Manag. 96, 167–183.

Brockway, D.G., Outcalt, K.W., 1998. Gap-phase regeneration in longleaf pine wiregrass ecosystems. Forest Ecol. Manag. 106, 125–139.

Chen, K., Bak, P., Jensen, M.H., 1990. A deterministic critical forest fire model. Phys. Lett. A 149, 207–210.

Cheng, Q., 1997. Multifractal modeling and lacunarity analysis. Math. Geol. 29, 919–932.

Cheng, Q., Agterberg, F.P., 1995. Multifractal modeling and spatial point processes. Math. Geol. 27, 831–845.

Dean, T.J., Jokela, E.J., 1992. A density-management diagram for slash pine plantations in the lower coastal plain. Southern J. Appl. Forest. 16, 178–185.

Drake, J.B., 1998. Characterizing and modeling spatial patterns of a longleaf pine savanna. M.S. Thesis. University of Central Florida, Orlando, FL, pp. 112.

Drake, J.B., Weishampel, J.F., 2000. Multifractal analysis of canopy height measures in a longleaf pine savanna. Forest Ecol. Manag. 128, 121–127.

Drossel, B., Schwabl, F., 1992. Self-organized critical forest-fire model. Phys. Rev. Lett. 69, 1629–1632.

Friend, A.D., Stevens, A.K., Knox, R.G., Cannell, M.R.G., 1997. A process-based, terrestrial biosphere model of ecosystem dynamics (Hybrid v3.0). Ecol. Modelling 95, 249–287.

Gilliam, F.S., Platt, W.J., 1999. Effects of long-term fire exclusion on tree species composition and stand structure in an old-growth Pinus palustris (longleaf pine) forest. Plant Ecol. 140, 15–26.

Grace, S.L., Platt, W.J., 1995. Neighborhood effects on juveniles in an old-growth of longleaf pine, *Pinus palustris*. Oikos 72, 99–105.

Harding, D.J., Blair, J.B, Garvin, J.B., Lawrence, W.T., 1994. Laser altimetry waveform measurement of vegetation canopy structure. In: Proceedings of the International Geoscience and Remote Sensing Symposium-IGARSS '94 ESA. Scientific and Technical Publication, Noordwijk, The Netherlands, pp. 1251–1253.

Holling, C., Peterson, G., Marples, P., Sendzimir, J., Redford, K., Gunderson, L., Lambert, D., 1996. Self-organization in ecosystems: lumpy geometries, periodicities and morphologies. In: Walker, B., Steffen, W. (Eds.), Global Change and Terrestrial Ecosystems. Cambridge University Press, Cambridge, England, pp. 346–384.

Kautz, R.S., 1998. Land use and land cover trends in Florida 1936–1995. Fla. Sci. 61, 171–187.

Lefsky, M.A., Harding, D., Cohen, W.B., Parker, G., Shugart, H.H., 1999. Surface lidar remote sensing of basal area and biomass in deciduous forests of eastern Maryland, USA. Remote Sens. Environ. 67, 83–98.

Lett, C., Silber, C., Barret, N., 1999. Comparison of a cellular automata network and an individual-based model for the simulation of forest dynamics. Ecol. Modelling 121, 277–293.

Lorimer, N.D., Haight, R.G. and Leary, R.A., 1994. The Fractal Forest: Fractal Geometry and Applications in Forest Science, NC-170, US Department of Agriculture, Forest Service, St. Paul, Minnesota, pp. 43.

Mach, J., Mas, F., Sagués, F., 1995. Two representations in multifractal analysis. J. Phys. A-Math. Gen. 28, 5607–5622.

Mandelbrot, B.B., 1988. An introduction to multifractal distribution functions. In: Stanley, H.E., Ostrowsky, N. (Eds.), Random Fluctuations and Pattern Growth: Experiments and Models. Kluwer Academic Publishers, Dordrecht, Netherlands, pp. 279–291.

Mandelbrot, B.B., Evertsz, J.G., 1991. Exactly self-similar left-sided multifractals. In: Bunde, A., Havlin, S. (Eds.), Fractals and Disordered Systems. Springer, New York, pp. 323–344.

McCay, D.H., 2000. Effects of chronic human activities on invasion of longleaf pine forests by sand pine. Ecosystems 3, 283–292.

Miller, C., Urban, D.L., 2000. Connectivity of forest fuels and surface fire regimes. Landscape Ecol. 14, 145–154.

Mladenoff, D.J., Baker, W.L., 1999. Spatial Modeling of Forest Landscape Change: Approaches and Applications. Cambridge University Press, Cambridge, p. 352.

Noel, J.M., Platt, W.J., Moser, E.B., 1998. Structural characteristics of old- and second-growth stands of longleaf pine (*Pinus palustris*) in the Gulf Coastal Region of the USA. Conserv. Biol. 12, 533–548.

Palik, B.J., Mitchell, R.J., Houseal, G., Pederson, N., 1997. Effects of canopy structure on resource availability and seedling responses in a longleaf pine ecosystem. Can. J. Forest Res. 27, 1458–1464.

Pielke, R.A., Avissar, R., Raupach, M., Dolman, A.J., Zeng, X., Denning, S., 1998. Interactions between the atmosphere and terrestrial ecosystems: influence on weather and climate. Glob. Change Biol. 4, 461–475.

Platt, W.J., 1999. Southeastern pine savannas. In: Anderson, R.C., Fralish, J.S., Baskins, J.M. (Eds.), The Savanna, Barren, and Rock Outcrop Communities of North America. Cambridge University Press, Cambridge, England, pp. 23–51.

Platt, W.J., Evans, G.W., Rathbun, S.L., 1988. The population dynamics of a long-lived conifer (*Pinus palustris*). Am. Nat. 131, 491–525.

Prihodko, L., Foresman, T., Knox, R.G., 1994. Improving ecological field studies: integrating GIS and stem mapping. Proceedings of Second International Conference/Workshop on Integrating Geographic Information systems and Environmental Modeling. Breckenridge, Colorado.

Rathbun, S.L., Cressie, N., 1994. A space-time survival point process for a longleaf pineforest in southern Georgia. J. Am. Stat. Ass. 89, 1164–1174.

Ricotta, C., 2000. From theoretical ecology to statistical physics and back: self similar landscape metrics as a synthesis of ecological diversity and geometrical complexity. Ecol. Modelling 125, 245–253.

Scheuring, I., Riedi, R.H., 1994. Application of multifractals to the analysis of vegetation pattern. J. Veg. Sci. 5, 489–496.

Schwartz, M.W., 1999. Choosing the appropriate scale of reserves for conservation. Annu. Rev. Ecol. Syst. 30, 83–108.

Shugart, H.H., 1996. The importance of structure in understanding global change. In: Walker, B., Steffen, W. (Eds.), Global Change and Terrestrial Ecosystems. Cambridge University Press, Cambridge, England, pp. 117–126.

Solé, R.V., Manrubia, S.C., 1995. Are rainforests self-organized in a critical state? J. Theor. Biol. 173, 31–40.

Spies, T.A., 1998. Forest structure: a key to the ecosystem. Northwest Sci. 72, 34–39.

Vedyushkin, M.A., 1994. Fractal properties of forest spatial structure. Vegetatio 113, 65–70.

Watt, A.S., 1947. Pattern and process in the plant community. J. Ecol. 35, 1–22.

Weishampel, J.F., Ranson, K.J., Harding, D., 1996. Remote sensing of forest canopies. Selbyana 7, 6–14.

Weishampel, J.F., Harding, D.J., Boutet, J.C., Drake, J.B., 1997. Analysis of laser altimeter waveforms for forested ecosystems of Central Florida. In: Narayanan, R.M., Kalshoven, J.E., Jr. (Eds.), Advances in Laser Remote Sensing for Terrestrial and Oceanographic Applications, Proceedings of SPIE, vol. 3059, pp.184–189.